HHS Public Access

Author manuscript

*Dev Biol*. Author manuscript; available in PMC 2021 August 01.

Published in final edited form as:

*Dev Biol*. 2020 August 01; 464(1): 1–10. doi:10.1016/j.ydbio.2020.05.009.

# FGF signaling promotes myoblast proliferation through activation of wingless signaling

**Kumar Vishal**[a], **TyAnna L. Lovato**[b], **Chandler Bragg**[a], **Maria B. Chechenova**[b], **Richard M. Cripps**[a,b,*]

[a]Department of Biology, San Diego State University, San Diego, CA, 92182, USA

[b]Department of Biology, University of New Mexico, Albuquerque, NM, 87131, USA

## Abstract

Indirect flight muscles (IFMs) are the largest muscles in *Drosophila* and are made up of hundreds of myonuclei. The generation of these giant muscles requires a large pool of wing disc associated adult muscle precursors (AMPs), however the factors that control proliferation to form this myoblast pool are incompletely known. Here, we examine the role of fibroblast growth factor (FGF) signaling in the proliferation of wing disc associated myoblasts. We find that the components of FGF signaling are expressed in myoblasts and surrounding epithelial cells of the wing disc. Next, we show that attenuation of FGF signaling results in a diminished myoblast pool. This reduction in the pool size is due to decreased myoblast proliferation. By contrast, activating the FGF signaling pathway increases the myoblast pool size and restores the proliferative capacity of FGF knockdown flies. Finally, our results demonstrate that the FGF receptor Heartless acts through up-regulating β-catenin/Armadillo signaling to promote myoblast proliferation. Our studies identify a novel role for FGF signaling during IFM formation and uncover the mechanism through which FGF coordinates with Wingless signaling to promote myoblast proliferation.

### Keywords

*Drosophila*; FGF; Imaginal wing disc; Myoblast proliferation; Wingless

## 1. Introduction

Muscle formation requires generation of the muscle precursor pool, followed by extensive proliferation, fusion and differentiation of the muscle precursor cells. Thus, one of the fundamental challenges in the field of muscle biology is to understand the mechanisms through which myoblast proliferation is controlled to attain proper muscle size. Studies carried out in vertebrates have highlighted the roles of various signaling pathways in the



*Corresponding author. Department of Biology, San Diego State University, San Diego, CA, 92182, USA. rcripps@sdsu.edu (R.M. Cripps).

Declaration of competeimg interest

The authors declare no competing or financial interests.

**Appendix A.:** Supplementary data

Supplementary data to this article can be found online at https://doi.org/10.1016/j.ydbio.2020.05.009.

regulation of myoblast proliferation. For example, in chick embryonic muscle BMP signaling promotes myoblast proliferation, whereas Sonic hedgehog (Shh) has an inhibitory effect on proliferation (Amthor et al., 1999). Similarly, work done in mouse myoblast derived cell lines has highlighted the antagonistic roles of BMP4 and Wnt signaling in the regulation of myoblast proliferation (Terada et al., 2013). Furthermore, FGF signaling promotes myoblast proliferation either alone (Gospodarowicz et al., 1976; Michailovici et al., 2014; Lu et al., 2015) or in combination with other signaling pathways (Kelvin et al., 1989). However, the way many of these pathways function in intact animals is not fully understood, and the molecular interactions of many of these pathways remains to be defined.

A comprehensive genetic dissection of the signaling networks regulating myoblast proliferation in the vertebrate model system is impeded by the presence of multiple ligands and receptors in individual signaling pathways. Therefore, a simple organism like *Drosophila*, with less redundant signaling components, can serve as a model system to explore the roles and crosstalk between signaling pathways during myoblast proliferation.

Indeed, studies performed in *Drosophila* adult myogenesis have provided an opportunity to dissect the mechanisms through which signaling networks regulate myoblast proliferation (Gunage et al., 2014; Aradhya et al., 2015). The indirect flight muscles (IFMs) are one of the largest adult muscles and are composed of hundreds of myoblasts (Fernandes et al., 2005; Gunage et al., 2014; Johnston et al., 2020). Importantly, the starting pool that generate these massive muscles consist of only 10 adult muscle progenitors (AMPs) at the end of embryogenesis (Bate et al., 1991; Gunage et al., 2014), and as a consequence these 10 AMPs must undergo rapid rounds of proliferation during the larval stages to generate approximately 2500 myoblasts in each wing imaginal disc within a short period of 96 h. This is followed by a second phase of AMP proliferation during the first day of pupal metamorphosis to form nascent muscle fibers (Fernandes et al., 2005). These fibers grow during the remaining period of metamorphosis to generate large IFMs (Zappia et al., 2016). More importantly, the proliferation of myoblasts overlaps with the development of the surrounding tissues (Garcia-Garcia et al., 1999; Calleja et al., 2000; Fernandes and Keshishian, 2005). Thus, neighboring tissues act through various signaling molecules to promote myoblast proliferation and subsequent muscle formation (Sudarsan et al., 2001; Gunage et al., 2014).

What signals are responsible for the proliferation of AMPs during *Drosophila* adult myogenesis? Previous studies have demonstrated that ectodermal Wingless (Wg) signaling controls myoblast pool size through maintenance of Vestigial expression in the wing disc associated AMPs (Sudarsan et al., 2001). Moreover, components of Wg signaling pathways are expressed in the disc and mediate the proliferation of AMPs in the third larval instar stage (Gunage et al., 2014). In addition to Wingless, Notch is also involved in the regulation of myoblast pool size (Anant et al., 1998; Bernard et al., 2006, 2010). Work done by Anant et al. (1998) showed that Notch is critical for the maintenance of AMPs in the proliferative phase. Similarly, absence of Notch signaling in AMPs results in premature muscle differentiation (Bernard et al., 2006). Furthermore, studies done by Gunage et al. (2014) have provided a detailed mechanism through which Notch signaling regulates the number of

AMPs. Notch mediates the communication between wing disc epithelial cells and AMPs to regulate myoblast proliferation in early larval instars.

How does crosstalk between signaling pathways impact myoblast proliferation? Studies have highlighted the importance of interaction between Notch and Wg signaling in the regulation of myoblast proliferation (Gunage et al., 2014). Initial amplification of the myoblast pool is triggered by activation of Notch in the AMPs. However, at the beginning of the third larval instar stage Wingless signaling acts though Numb to block Notch receptor activity (Frise et al., 1996) and attain the proliferative role. Thus, the interplay of Notch and Wg is critical for rapid division of the AMPs in the wing disc. Although these studies have increased our knowledge about regulation of myoblast proliferation, it is important to explore how Notch and Wg interact with other disc associated signaling molecules to control myoblast proliferation.

Emori and Saigo (1993) analyzed the expression of the two FGF receptor genes during development and showed that *heartless (htl)*, but not *breathless*, was expressed in the wing disc associated myoblasts. Moreover, previous studies highlighted the role of Heartless in the specification of founder cell and regulation of fiber number during adult abdominal myogenesis (Dutta et al., 2005), and FGF ligands regulate the number of adult abdominal muscles (Sarkissian et al., 2016). Furthermore, Htl signaling controls the number of leg disc associated myoblasts and activates one of the Wingless targets, *ladybird*, to regulate fiber formation (Maqbool et al., 2006). Taken together, these studies indicate that FGF signaling influences different aspects of adult myogenesis, however the role of FGF signaling in AMP proliferation remains unexplored.

In this manuscript, we investigate how FGF signaling regulates proliferation of wing disc associated myoblasts. We demonstrate that components of the FGF signaling cascade are expressed in AMPs and the surrounding epithelial cells of the wing disc during myoblast proliferation. Moreover, blocking FGF signaling causes a severe reduction the number of AMPs, due to impaired myoblast proliferation. By contrast, activating FGF signaling significantly increases myoblast number and rescues the defect in the myoblast pool. To further understand the mechanism of FGF regulating myoblast proliferation, we examined the cross talk between FGF and Wingless signaling. We find that Heartless activates β-catenin signaling to promote myoblast proliferation. Collectively, our data support a model that highlights the role of FGF signaling and its interaction with the Wingless pathway in the control of myoblast proliferation. These findings will help us better understand the role of crosstalk between signaling molecules during vertebrate myogenesis.

## 2. Materials and methods

### 2.1. Fly stocks and genetics

The following fly stocks were obtained from the Bloomington *Drosophila* Stock Center (BL) or the Vienna *Drosophila* RNAi Center (VDRC): *UAS-thisbe RNAi* (VDRC, 102441), *ap-GAL4/CyO* (BL, 3041), *UAS-htl RNAi* (BL, 35024), *UAS-dn htl* (BL, 5366), *UAS-htl ca* (BL, 5367), *UAS-pointed RNAi* (BL, 35038), *UAS-MAPkinase ca* (BL, 59006), *UAS-arm$^{S10}$* (BL, 4782), *thisbe-Gal4* (BL, 77475), *UAS-nls GFP* (BL, 4775) and *UAS-GFP*

*RNAi* (BL, 9331). The following fly lines were generated in our laboratory using genetic crosses. *UAS-MAPkinase ca; UAS-htl RNAi* (for rescue of *htl* RNAi phenotype), *UAS-GFP RNAi; UAS-htl RNAi* (control for rescue experiment), and *UAS-arm* $^{S10}$*; UAS-htl RNAi* (rescue of *htl* RNAi by activated β-catenin). Thisbe lines (*ths*$^{02026}$*/CyO, Actin-GFP* and *Df(2R) ths238/CyO, Actin-GFP* were a gift from the Stathopoulos laboratory (Stathopoulos et al., 2004; Kelvin et al., 1989; Kadam et al., 2009).

### 2.2. Immunohistochemistry and microscopy

Wing discs from wandering third instar larvae were dissected in PBS, fixed in 4% formaldehyde followed by immunolabeling. Wing disc associated myoblasts were labeled using guinea pig anti-Ebd1 (1:2000; Yashi Ahmed) or rabbit anti-MEF2 (1:1000, generated here). Myoblast proliferation was monitored using rabbit anti-PH3 (1:100; Millipore). Cell death was examined using rabbit anti-Cleaved Caspase-3 (1:100; Cell Signaling). Premature differentiation was studied using Alexa-Phalloidin (Invitrogen). Localization studies were done using guinea pig anti-Htl (1:400; Christian Klambt), rabbit anti-Dof (1:200; Maria Leptin), mouse anti-GFP (1:10; DSHB), and chick anti-βgal (1:1000, ICL lab). Mouse anti-β Catenin (1:20; DSHB) was used to analyze the readout of Wg signaling. Wg ligand expression was visualized using anti-Wg (1:10; DSHB). Alexa 488 and Alexa 546 secondary antibodies (Molecular Probes) were used in this study. Samples were mounted in mounting media and imaged with an Olympus FV 3000 confocal microscope. Images were processed using Olympus Life Science software and Adobe Photoshop CC 2018.

### 2.3. Quantification and data analysis

All quantitative data were generated from 6 to 10 flies of each genotype. Quantifications were performed in Image J, and the results were imported into Graphpad Prism 6.0 software for the generation of graphs and statistical analysis. We used the column statistics function to determine statistically significant sample sizes and normality. All error bars represent the mean ± SEM. Statistical significances were determined using Student's t-tests, and Mann–Whitney tests.

Myoblasts were visualized by anti-MEF2 and anti-Ebd1 antibodies. Previous studies have shown that both *Ebd1* and *Mef2* have overlapping expression pattern in the late third instar wing disc (Benchanabe et al., 2011). Counting the total number of myoblasts in all the samples for all the images presented here was not practical, therefore myoblast pools were analyzed in a representative confocal plane which had maximum myoblast expanse. Quantification was performed using two different parameters: a) Myoblast number was determined by counting the total number of MEF2 or Ebd1 positive myoblasts in a single confocal plane of the wing disc; b) Myoblast area was measured as a fraction of the total area occupied by the wing disc. While each of these approaches do not determine to the total number of myoblasts per imaginal disc, the data generated are highly representative of the total myoblast pool. Indeed, when we counted the total number of myoblasts in a representative experiment, the overall conclusions were the same (see Fig. S3).

Myoblast proliferation was determined by calculating the fraction of proliferating myoblasts in the notum region of late third larval instar wing imaginal discs. The read-out of Wg

signaling was monitored by measuring the fraction of strongly labeled nuclear β-Catenin (+)/MEF2 (+) myoblasts. 6–10 samples of each genotype were analyzed.

Corrected total fluorescence (CTF): To monitor the effect of manipulating Htl signaling on Arm nuclear protein levels, we compared the fluorescence intensities of Arm/βcat in control and experimental samples using the CTF method (McCloy et al., 2014; Green et al., 2016; Vishal et al., 2018). The fluorescence intensity was measured in a single optical section of MEF2-positive adult muscle precursors. Background measurement was done in an area outside the wing disc. Corrected total fluorescence (CTF) was calculated as follows: CTF = Integrated density- (area of selected cell x mean fluorescence of background). All quantifications were carried using the measurement function of Image J and data was analyzed in GraphPad Prism 7.

### 2.4. MEF2 protein synthesis for antibody generation

The coding sequence of *Mef2* was cloned into the pEXP1-DEST vector (ThermoFisher V96001) utilizing Gateway Technology via pDONR221 (ThermoFisher 12536017). A positive clone was then transformed into BL21 (DE3) competent cells (ThermoFisher C600003). To produce His-tagged MEF2 protein, BL21 (DE3) transformants were grown overnight with shaking at 37 °C in 50 ml liquid LB media containing antibiotic. The overnight culture then was diluted 25 times in 2 L of fresh LB media with antibiotic and was grown to an $OD_{600}$ of 0.5. Protein synthesis was induced with 1 mM IPTG and returned to the shaking incubator for three additional hours. Cells were collected by centrifugation at 3000 × *g* for 15 min at 4 °C and resuspended in 200 ml of denaturing equilibration buffer (50 mM Na-phosphate pH7.0, 300 mM NaCl, 8 M urea) and incubated at room temperature with rotation for 1 h. Lysate was centrifuged at 10,000 × *g* at 4 °C for 20 min. The supernatant was transferred to a flask and 1 ml of Talon Metal Affinity Resin (Takara 635501), washed with denaturing equilibration buffer, was added and incubated at 4 °C with rotation for 1 h. Lysate was centrifuged at 700×*g* for 10 min at 4 °C and the supernatant was removed and discarded. Resin was washed with denaturing equilibration buffer and packed into a 10 ml column (BioRad 7311550). The column was washed with 5 ml of denaturing equilibration buffer and eluted with 5 ml of the same buffer containing 150 mM imidazole. 500 μl fractions were collected and analyzed by SDS page.

### 2.5. Polyclonal MEF2 antibody production

Two New Zealand white rabbits were injected with 500 μl of Freund's Complete Adjuvant (Sigma-Aldrich F5881) containing 500 μg of MEF2 protein at ten sites. A small blood draw was carried out 4 weeks later to check progress and a booster injection of 100 μg of MEF2 protein in 200 μl of Freund's Incomplete Adjuvant (Sigma-Aldrich 344291) was injected at four sites. Two weeks later 50 ml of blood was drawn to check titer, after which a second booster was administered a week later. Four weeks later the final blood draw was obtained. Serum was collected by allowing the blood to coagulate at room temperature for 30 min and then centrifuged at 2000×*g*. The supernatant was transferred to a clean tube and analyzed by immunohistochemistry using a concentration of 1:1000. Approximately 50 ml of blood was collected for each blood draw. There was no need for complete exsanguination and the

rabbits were both adopted. The protocol was IACUC approved (protocol number 18–200741-MC) prior to commencing the work.

## 3. Results

### 3.1. Expression of FGF signaling pathway components in the wing disc

To define a role for the FGF signaling pathway in the regulation of myoblast proliferation, we first sought to examine the expression of different components of the pathway in third instar wing imaginal discs. For this purpose, we performed immunolabeling studies using a myoblast marker (anti-MEF2 or anti-Ebd), enhancer trap reporters, or FGF-specific antibodies.

First, we monitored the localization of FGF ligand, Thisbe (Ths), in *ths* > *nls-GFP* larvae. This *ths-Gal4* line has previously been shown to recapitulate *ths* expression (Wu et al., 2017). At a confocal plane corresponding to the epithelial cells of the notum (located below the myoblast layer), we observed robust expression of the GFP reporter, but no accumulation of the myoblast marker MEF2 (Fig. 1A). By contrast, at a shallower confocal plane we identified MEF2-positive myoblasts, which did not express the GFP reporter (Fig. 1B). These results showed that the GFP reporter is expressed only in the epithelial cells of the wing disc, and GFP is absent from MEF2-positive myoblasts. Single orthogonal views through the wing disc notum further demonstrated that *ths*-expressing cells lie adjacent to the layer of MEF2-positive myoblasts (Fig. 1C, C'). Therefore, while *ths* is not expressed in the myoblasts, this FGF ligand is expressed in a location where it can impact the myoblasts.

Next, we examined the expression of components of the FGF pathway in myoblasts. The FGF receptor was detected using anti-Htl serum and was localized around all the wing disc associated myoblasts nuclei (Fig. 1D–F), in a location consistent with its accumulation at the plasma membrane. This finding supports those of Emori and Saigo (1993) who demonstrated that Htl is expressed in the wing disc myoblasts. Next, we examined other downstream components of FGF signaling. Downstream of FGF (Dof) is an intracellular adaptor protein which binds to Htl and activates downstream effectors of the FGF pathway (Vincent et al., 1998; Michelson et al., 1998), and its accumulation was examined using anti-Dof antibody. Our immunofluorescent analysis showed that Dof protein was uniformly expressed in myoblasts throughout the wing disc (Fig. 1G–I). Finally, we monitored expression of *pointed* (*pnt)*, whose gene product acts downstream of MAP Kinase and functions as a positive regulator of the FGF pathway (O'Neill et al., 1994). A *pnt-lacz* reporter construct was active in most of the wing disc associated myoblast nuclei (Fig. 1J–K). Collectively, our results indicate that *htl*, *Dof* and *pnt* have highly overlapping expression patterns in rapidly dividing adult myoblasts. Furthermore, the proximity of Thisbe expressing cells to the layer of actively proliferating myoblasts suggests that Thisbe might impact AMP development.

### 3.2. Manipulating the FGF pathway affects myoblast pool size

Next, we investigated the role of FGF signaling in the myoblasts. To achieve this, we manipulated components of the FGF signaling cascade and examined the effects on

myoblasts. To assess myoblast number, we determined both the total area of the disc covered by myoblasts, and the number of myoblasts in a representative plane of the wing imaginal disc.

First, we analyzed how absence of the FGF ligand, Thisbe (Ths), impacted the myoblast pool compared to controls. In controls, the myoblasts are readily apparent (Fig. 2A), and cover approximately 25% of the area of the whole disc (Fig. 2C). In a single plane, we count an average of ~830 myoblasts (Fig. 2D). By contrast, *ths* mutants have a significantly reduced coverage of the wing disc as compared to wild type flies (Fig. 2B and C), and there was an approximately 30% reduction in myoblast number in *ths* mutant flies (Fig. 2D). To confirm these data, we knocked down *ths* expression in the wing disc epithelium using the GAL4/UAS system (Brand and Perrimon, 1993). Again, compared to controls we noted severe reduction in the number of myoblasts in *ap* > *ths RNAi* discs (Fig. 2E–H). In contrast, disrupting the other FGF ligand, Pyramus, did not alter myoblast pool size (Fig. S1). Collectively, these results demonstrate that the FGF ligand Thisbe regulates myoblast number.

Next, we determined the role of the Htl receptor in the regulation of myoblast pool size. To achieve this, we expressed a dominant negative *htl* allele in the myoblasts, and in a separate experiment we knocked down *htl* expression using RNAi. Abrogation of *htl* function using each of these approaches significantly lowered the myoblast number, although the effect was stronger in *1151* > *htl RNAi* discs (Fig. 2I–L, Fig. S2). These results were further corroborated by the quantification of the entire myoblast population in control and *1151* > *htl RNAi* samples (Fig. S3). To further test if Htl regulates myoblast number, we activated the FGF pathway using a constitutively activated form of Htl. Interestingly, *1151* > *htl ca* wing imaginal discs had significantly higher myoblast number and area as compared to wild type flies (Fig. 2M–P). These observations clearly demonstrate that perturbing Htl function affects the number of wing-disc associated myoblasts.

To further dissect the role of FGF signaling, we examined the effect of disrupting a downstream effector of the pathway using 115 > *pnt RNAi* larvae. Our results indicated that disrupting Pnt function caused a similar reduction in the myoblast pool size as observed in the case of *1151* > *htl RNAi* or *ap* > *ths RNAi* flies (Fig. 2Q–T). Together, our results provide strong evidence for a role of the FGF signaling pathway in the regulation of myoblast pool size.

### 3.3. Heartless controls myoblast number through promoting proliferation

To gain insight into how FGF signaling regulates myoblast number, we examined apoptosis, premature muscle differentiation, and myoblast proliferation in the wing discs. To determine if Htl promotes increased myoblast number through preventing apoptosis, we monitored cleaved Caspase-3 staining in wing disc associated myoblasts of control and *1151* > *htl RNAi* flies. We hardly observed any caspase positive myoblasts in either group, suggesting that Htl does not regulate myoblast number through preventing apoptosis (Fig. S4). Next, to test the possibility that the reduced pool is due to differentiation of wing disc myoblasts into muscles at the wandering third larval instar stage, we compared F-actin accumulation in control and experimental flies. We did not observe F-actin labelling in the wing that might

suggest muscle formation in disc associated myoblasts of either control or experimental genotypes (Fig. S5).

Finally, we tested the hypothesis that Htl controls myoblast pool size through proliferation. We compared myoblast proliferation between *1151-GAL4/+* control and *1151 > htl RNAi* flies by staining for phosphohistone H3 (PH3), and then calculating the proportion of Ebd-positive myoblasts that were also PH3-positive in single confocal planes. Our results indicated that about 9% of wing disc associated myoblasts of control larvae were PH3 positive, whereas *1151 > htl RNAi* larval wing discs had a significantly lower percentage (4.9%) of PH3 positive myoblasts (Fig. 3A–G). By contrast, activating Htl signaling resulted in a significantly higher percentage (13.1%) of PH3 positive myoblasts as compared to control flies (Fig. 3H–N). Together, our results provide strong evidence that FGF expands the number of wing disc associated myoblasts through promoting proliferation.

### 3.4. Heartless acts through the MAP kinase pathway to control myoblast number

Previous studies have shown that the RTK/FGF signaling pathway in *Drosophila* exhibits linearity during the regulation of numerous developmental events (Shilo, 2014). Therefore, we tested the hypothesis that Heartless/FGF signaling acts in a similar fashion to regulate myoblast number. The idea of linearity is supported by our above-mentioned results in which we have demonstrated that loss of one of the downstream targets of the FGF/MAP kinase pathway, Pointed, mimics the *1151 > htl RNAi* or *ap > ths RNAi* associated defects.

To test the linearity of the FGF pathway in regulating proliferation, we determined whether MAP kinase acts downstream of Htl to regulate myoblast pool size. To achieve this, we over-expressed an activated form of MAP kinase in the genetic background of *1151 > htl RNAi* to see if the activated MAP kinase would rescue the reduction in myoblasts arising from *htl* knockdown. Our results indicate that overexpression of activated MAP kinase rescued the number of wing disc associated myoblasts in *1151 > htl RNAi* flies. The total number of myoblasts present in *1151 > htl RNAi* alone was 272 in the confocal plane with the largest number of myoblasts, whereas re-introduction of activated MAP kinase increased the number of myoblasts to 931, which is similar to *1151/+* controls. By contrast, there was no significant difference in the number of myoblasts between *1151 > GFP RNAi; htl RNAi*, and *1151 > htl RNAi* samples, indicating that using two UAS lines does not dilute the effectiveness of the *1151-Gal4* driver (Fig. 4 C, D, F). Taken together, these results provide strong evidence that Htl acts through MAP kinase to regulate myoblast pool size.

### 3.5. Heartless signaling activates Wingless signaling

The output of the Wingless (Wg) signaling cascade is dictated by cytoplasmic versus nuclear localization/accumulation of the transcriptional cofactor Armadillo (Arm)/β-Catenin (Bejsovec, 2006; Saito-Diaz et al., 2013). In the absence of a Wg signal, a group of proteins termed the destruction complex (Axin, APC and Shaggy) phosphorylates cytoplasmic Arm/β-Catenin. This initiates its destruction by the proteasomal complex, thereby preventing the transcription of Wg responsive genes (Swarup and Verheyen, 2012). On the other hand, binding of the Wg ligand to the Frizzled (Fz) receptor results in either destruction or inactivation of the destruction complex (Li et al., 2012; Gerlach et al., 2014). These events

result in cytoplasmic Arm/β-Catenin accumulation, followed by its nuclear translocation and the subsequent transcriptional activation of Wingless target genes.

Comparison of our findings with previous studies (Gunage et al., 2014) indicated that both the FGF and Wg signaling cascades have overlapping expression at the third larval instar stage. Furthermore, both these pathways share a similar role in the regulation of myoblast number. Therefore, we next asked whether there is crosstalk between pathways during the amplification of the myoblast pool. Toward this end, our first step was to examine whether Htl signaling activates Wingless ligand expression to regulate myoblast number. Previous studies have shown that Wg is expressed in a broad stripe of notal epithelial cells adjacent to the myoblast population (Swarup and Verheyen, 2012; Gunage et al., 2014). Importantly, we did not observe any differences in Wg accumulation between the epithelial cells of control and *1151 > htl RNAi* wing discs (Fig. S6). Thus, Htl signaling does not seem to control the expansion of the myoblast pool size through activation of Wg ligand expression.

Next, we examined whether manipulation of Htl signaling impacts nuclear accumulation of β-catenin (as a read-out of the Wingless pathway) in the wing disc associated myoblasts. Previous studies have used anti-β-Catenin antibody to monitor Wg signaling (Gunage et al., 2014). Using the same antibody and analyzing confocal planes that include myoblasts but not underlying epithelial cells, we observed that 22% of the myoblast nuclei of control flies have high nuclear β-catenin staining (Fig. 5, A–C, J). Abrogation of Htl resulted in a severe reduction in nuclear accumulation of β-Catenin, with only 7% of myoblast nuclei enriched for β-Catenin (Fig. 5D–F, J). By contrast, activation of Htl signaling in *1151 > htl ca* discs caused a massive surge in the nuclear enrichment of β-Catenin (Fig. 5G–I, J). Quantification showed that *1151 > htl ca* flies had 72% strongly labeled β-Catenin (+)/MEF2 (+) nuclei, compared to 22% in control flies (Fig. 5J). Moreover, we observed significant differences in the fluorescence intensity of β-Catenin positive myoblasts in both *1151 > htl RNAi* and *1151 > htl ca* samples as compared to controls (Fig. 5K). Together, these results clearly demonstrate that activation of the Htl pathway causes activation of β-Catenin signaling.

To determine if Htl acts through the Wg signaling pathways to promote myoblast proliferation, we examined whether ectopic activation of Wg signaling could rescue the defects in myoblast pool size observed in the case of *1151 > htl RNAi* flies. To achieve this, we over-expressed an activated form of Armadillo ($Arm^{S10}$) in the genetic background of larvae with *htl* expression knocked down. Compared to control (Fig. 6A) and *htl* knockdown (Fig. 6B), activating Armadillo in the background of 1151 > *htl RNAi* resulted in rescue of the number of myoblasts (Fig. 6C) as compared to *1151 > htl RNAi* alone. Expression of activated Armadillo in a wild-type background did not affect myoblast number (Fig. 6D). Quantification of the number of myoblasts in control and experimental animals indicated that expression of $arm^{S10}$ restored the myoblast pool size to wild-type levels (Fig. 6E). Furthermore, we found that expressing *arm RNAi* in the genetic background of *1151 > htl RNAi* resulted in a drastic reduction in the number of wing disc associated myoblasts as compare to either *1151 > htl RNAi* or *1151 > arm RNAi* alone (Fig. S7). Taken together, our results demonstrate that Htl interacts with the Wg signaling pathway to regulate myoblast number.

## 4. Discussion

In this manuscript, we elucidate a role for FGF signaling in the regulation of adult myoblast pool size during IFM myogenesis. First, we show that components of FGF signaling are expressed in the AMPs and the surrounding epithelial cells of the wing disc notum. Next, we demonstrate that FGF signaling regulates myoblast proliferation to control the size of the myoblast pool. Furthermore, we demonstrate that FGF-mediated regulation of myoblast proliferation is achieved through activation of β-Catenin signaling. Collectively, our results demonstrate the role of FGF mediated communication between wing disc epithelial cells and myoblasts during myoblast proliferation. More importantly, our data highlight the importance of crosstalk between FGF and β-Catenin signaling in the regulation of myoblast pool size.

Studies done in vertebrates have also reported a role for FGF signaling in the regulation of myoblast proliferation. Work done by Jones et al. (2001) on mouse hind limb muscle cell lines demonstrated the requirement of FGFRs in myoblast proliferation. Similarly, FGF-ERK signaling is involved in maintaining the myoblasts in a proliferative phase in chick embryonic muscles (Michailovici et al., 2014). Furthermore, other studies have indicated the proliferative effects of FGF13, FGF6 and FGF2 ligands during muscle development and regeneration (Lu et al., 2015; Yablonaka-Reuveni and Rivera, 1997; Floss et al., 1997). Our studies are consistent with these previous findings and underline the utility of the *Drosophila* system to uncover basic aspects of myoblast biology. Importantly, many of the *Drosophila* signaling components are single copy in the haploid genome, or paralogs show non-overlapping patterns of gene expression, enabling us to genetically dissect this process more easily in *Drosophila*.

Apart from FGF signaling, additional signaling pathways are known to stimulate myoblast proliferation. In *Drosophila*, Wingless and Notch play crucial roles in the amplification of the wing disc associated myoblast pool (Sudarsan et al., 2001; Gunage et al., 2014). Similarly, BMP signaling promotes myoblast proliferation in the chick embryonic muscles (Amthor et al., 1999). Likewise, activation of Wnt signaling enhances the proliferation of skeletal muscle precursor cells in the chick hindlimb muscles (Takata et al., 2007). Furthermore, EGF signaling positively regulates proliferation in ovine fetal myoblasts (Harper and Buttery, 2001). How these different pathways might converge to achieve the same end goal is not fully understood, however our studies for the first time demonstrate crosstalk between FGF and Wingless signaling in myoblast proliferation, suggesting that multiple signals might converge on the same regulatory module. Moreover, as the myoblasts continue their proliferation and differentiate during the pupal stage, additional regulatory signals and cross-talk may occur.

Studies in non-muscle tissues have reported crosstalk between signaling pathways during the regulation of progenitor cell populations (Xu et al., 2011; Ren et al., 2010; Lu et al., 2019; Armstrong et al., 2018). For example, Wingless, JAK-STAT and EGFR pathways work in a coordinated manner to regulate proliferation of intestinal stem cells in the *Drosophila* midgut (Xu et al., 2011). Similarly, studies done in the *Drosophila* testis demonstrate that Dpp signaling activates EGFR signaling to promote proliferation of cyst stem cells (Lu et

al., 2019). Furthermore, collaboration between Notch and Hedgehog signaling dictates the proliferation of *Drosophila* wing pouch cells (Casso et al., 2011). Clearly, the collaborative effects of distinct signaling pathways is a common theme in the regulation of development and extends to the control of myoblast proliferation.

Our data also underline the importance of communication between germ layers in myoblast proliferation, where ectodermal tissues (the wing disc epithelium) signal through the FGF ligand Thisbe to dictate the size of the wing disc associated myoblast pool. These findings are reminiscent of the roles of Notch and Wg signaling in controlling myoblast proliferation in *Drosophila* (Gunage et al., 2014). More broadly, evidence of a role for an ectoderm-derived signal regulating myoblast proliferation stems from work done in chick embryonic muscle (Bonner, 1978). Later on, studies done in rat lumbrical muscles have further substantiated the role of neuronal signals in myoblast proliferation (Ross et al., 1987).

Our study provides novel insights into regulation of AMP number during IFM formation, as well as raising several further questions. Our results indicate that activating Heartless signaling drastically increases the expression of nuclear β-catenin, whereas disrupting Heartless function reduces nuclear β-catenin levels. Moreover, activation of Wingless signaling rescues the defects in myoblast pool observed in case of *1151 > htl RNAi* flies. Collectively, these results demonstrate that Heartless acts through Wingless signaling to control myoblast number. However, it important to further dissect the mechanism through which Heartless interacts with β-Catenin signaling, which could occur in two possible ways: in one scenario, Heartless may downregulate the expression of β-Catenin destruction complex components, thereby activating β-Catenin signaling; alternatively, it is possible that Heartless directly regulates β-Catenin expression and its nuclear transport to regulate proliferation. It is also possible that these pathways may partly act independently to influence myoblast proliferation. In either of the above-mentioned scenarios, crosstalk between Heartless and β-Catenin signaling is crucial for the regulation of myoblast proliferation.

It will also be important to determine if FGF signaling interacts with Notch signaling to regulate myoblast proliferation. Components of both Notch and FGF signaling cascades are expressed in an overlapping pattern in the wing imaginal disc. More importantly, both these pathways are required for the amplification of the wing disc associated myoblast pool. Interestingly, Bernard et al. (2010) have predicted *pointed* as one of the potential targets of Notch signaling. Therefore, it is possible that Notch stimulates FGF signaling by transcriptionally activating *pointed* to regulate myoblast proliferation. Alternatively, FGF and Notch may act in parallel to activate the downstream target gene expression to promote myoblast proliferation. Our future studies will be aimed at testing these possibilities.

How is the maximum number of wing disc-associated myoblasts controlled? We demonstrate here that constitutively activated Htl causes significant expansion of the myoblast pool above that normally observed in control wing imaginal discs, however expression of downstream factors in the pathway does not cause the same over-accumulation of myoblasts. It is likely that activation of the Htl signaling pathway has additional effects

beyond those described here, and it will be interesting to identify how supernumerary myoblasts might be formed.

Finally, recent studies have reported the existence of cells resembling muscle satellite cells in *Drosophila* (Chaturvedi et al., 2017; Boukhatmi and Bray, 2018). However, the factors that regulate satellite cell proliferation in *Drosophila* are largely unknown. Work done in vertebrate myogenesis has highlighted FGF as one of the major factors regulating satellite proliferation (reviewed in Pawlikowski et al., 2017). Since adult AMPs share similarity with satellite cells, it will be vital to examine whether FGF signaling regulates satellite cell proliferation in *Drosophila*.

## Supplementary Material

Refer to Web version on PubMed Central for supplementary material.

## Acknowledgements

We are extremely grateful to the numerous individuals who shared reagents essential for this work: Maria Leptin, Christian Klambt, Yashi Ahmed and Angela Stathopoulos. This work was supported by GM061738 awarded by the NIH to RMC. Additional support was provided by funds from the University of New Mexico (UNM) Department of Biology, and from NCI grants U54 CA132384 and U54 CA132379. We acknowledge technical support from the UNM Department of Biology's Molecular Biology Facility, supported by P20 GM103452 from the Institute Development Award (IDeA) Program of NIGMS.

## References

Amthor H, Christ B, Patel K, 1999 A molecular mechanism enabling continuous embryonic muscle growth - a balance between proliferation and differentiation. Development 126, 1041–1053. [PubMed: 9927604]

Anant S, Roy S, VijayRaghavan K, 1998 Twist and Notch negatively regulate adult muscle differentiation in Drosophila. Development 125, 1361–1369. [PubMed: 9502718]

Aradhya R, Zmojdzian M, Da Ponte JP, Jagla K, 2015 Muscle niche-driven insulin-notch-myc cascade reactivates dormant adult muscle precursors in Drosophila. eLife 4, e08497. [PubMed: 26650355]

Armstrong AR, Drummond-Barbosa D, 2018 Insulin signaling acts in adult adipocytes via GSK-3β and independently of FOXO to control *Drosophila* female germline stem cell numbers. Dev. Biol 440, 31–39. [PubMed: 29729259]

Bate M, Rushton E, Currie DA, 1991 Cells with persistent twist expression are the embryonic precursors of adult muscles in Drosophila. Development 113, 79–89. [PubMed: 1765010]

Bejsovec A, 2006 Flying at the head of the pack: Wnt biology in Drosophila. Oncogene 25, 7442–7449. [PubMed: 17143288]

Benchabane H, Xin N, Tian A, Hafler BP, Nguyen K, Ahmed A, Ahmed Y, 2011 Jerky/Earthbound facilitates cell-specific Wnt/Wingless signalling by modulating beta-catenin-TCF activity. EMBO J. 30, 1444–1458. [PubMed: 21399610]

Bernard F, Dutriaux A, Silber J, Lalouette A, 2006 Notch pathway repression by vestigial is required to promote indirect flight muscle differentiation in Drosophila melanogaster. Dev. Biol 295, 164–177. [PubMed: 16643882]

Bernard F, Krejci A, Housden B, Adryan B, Bray SJ, 2010 Specificity of Notch pathway activation: twist controls the transcriptional output in adult muscle progenitors. Development 137, 2633–2642. [PubMed: 20610485]

Bonner PH, 1978 Nerve-dependent changes in clonable myoblast populations. Dev. Biol 66, 207–219. [PubMed: 751836]

Boukhatmi H, Bray S, 2018 A population of adult satellite-like cells in Drosophila is maintained through a switch in RNA-isoforms. Elife 7, 1–24.

Brand AH, Perrimon N, 1993 Targeted gene expression as a means of altering cell fates and generating dominant phenotypes. Development 118, 401–415. [PubMed: 8223268]

Calleja M, Herranz H, Estella C, Casal J, Lawrence P, Simpson P, Morata G, 2000 Generation of medial and lateral dorsal body domains by the *pannier* gene of *Drosophila*. Development 127, 3971–3980. [PubMed: 10952895]

Casso DJ, Biehs B, Kornberg TB, 2011 A novel interaction between hedgehog and Notch promotes proliferation at the anterior-posterior organizer of the Drosophila wing. Genetics 187, 485–499. [PubMed: 21098717]

Chaturvedi D, Reichert H, Gunage RD, VijayRaghavan K, 2017 Identification and functional characterization of muscle satellite cells in Drosophila. eLife 6, e30107. [PubMed: 29072161]

Dutta D, Shaw S, Maqbool T, Pandya H, Vijayraghavan K, 2005 Drosophila Heartless acts with Heartbroken/Dof in muscle founder differentiation. PLoS Biol. 3 (10), e337. [PubMed: 16207075]

Emori Y, Saigo K, 1993 Distinct expression of two Drosophila homologs of fibroblast growth factor receptors in imaginal discs. FEBS Lett. 332, 111–114. [PubMed: 8405423]

Fernandes JJ, Keshishian H, 2005 Motoneurons promote proliferation and patterning during adult myogenesis in Drosophila. Dev. Biol 277, 493–505. [PubMed: 15617689]

Fernandes JJ, Atreya KB, Desai KM, Hall RE, Patel MD, 2005 A dominant negative form of Rac1 affects myogenesis of adult thoracic muscles in Drosophila. Dev. Biol 285, 11–27. [PubMed: 16125691]

Floss T, Arnold HH, Braun T, 1997 A role for Fgf-6 in skeletal muscle regeneration. Genes Dev 11, 2040–2051. [PubMed: 9284044]

Frise E, Knoblich JA, Younger-Shepherd S, Jan LY, Jan YN, 1996 The Drosophila numb protein inhibits signaling of the Notch receptor during cell-cell interaction in sensory organ lineage. Proceedings of the National Academy of Sciences of USA 93, 11925–11932.

Garcia-Garcia MJ, Ramain P, Simpson P, Modolell J,J, 1999 Different contributions of Pannier and Wingless to the patterning of the dorsal mesothorax of *Drosophila*. Development 126, 3523–3532. [PubMed: 10409499]

Gerlach JP, Emmink BL, Nojima H, Kranenburg O, Maurice MM, 2014 Wnt signalling induces accumulation of phosphorylated beta-catenin in two distinct cytosolic complexes. Open Biol 4, 140120. [PubMed: 25392450]

Gospodarowicz D, Weseman J, Moran JS, Lindstron J, 1976 Effect of a fibroblast growth factor on the division and fusion of bovine myoblasts. J. Cell Biol 70, 395–405. [PubMed: 945805]

Green N, Odell N, Zych M, Clark C, Wang Z-H, Biersmith B, Bajzek C, Cook KR, Dushay MS, Geisbrecht ER, 2016 A common suite of coagulation proteins function in Drosophila muscle attachment. Genetics 204, 1075–1087. [PubMed: 27585844]

Gunage RD, Reichert H, VijayRaghavan K, 2014 Identification of a new stem cell population that generates Drosophila flight muscles. Elife 3, e03126.

Harper JM, Buttery PJ, 2001 Effects of EGF receptor ligands on fetal ovine myoblasts. Domest. Anim. Endocrinol 20, 21–35. [PubMed: 11164331]

Johnston JS, Zapalac ME, Hjelmen CE, 2020 Flying high-muscle-specific under replication in *Drosophila*. Genes 11 (3), 246.

Jones NC, Fedorov YV, Rosenthal RS, Olwin BB, 2001 ERK1/2 is required for myoblast proliferation but is dispensable for muscle gene expression and cell fusion. J. Cell. Physiol 186, 104–115. [PubMed: 11147804]

Kadam S, McMahon A, Tzou P, Stathopoulos A, 2009 FGF ligands in Drosophila have distinct activities required to support cell migration and differentiation. Development 136 (5), 739–747. [PubMed: 19158183]

Kelvin DJ, Simard G, Connolly JA, 1989 FGF and EGF act synergistically to induce proliferation in BC3H1 myoblasts. J. Cell. Physiol 138, 267–272. [PubMed: 2783932]

Li VS, Ng SS, Boersema PJ, Low TY, Karthaus WR, Gerlach JP, Mohammed S, Heck AJ, Maurice MM, Mahmoudi T, et al., 2012 Wnt signaling through inhibition of beta-catenin degradation in an intact axin1 complex. Cell 149, 1245–1256. [PubMed: 22682247]

Lu H, Shi X, Wu G, Zhu J, Song C, Zhang Q, Yang G, 2015 FGF13 regulates proliferation and differentiation of skeletal muscle by down-regulating Spry1. Cell Prolif 48 (5), 550–560. [PubMed: 26230950]

Lu Y, Yao Y, Li Z, 2019 Ectopic Dpp signaling promotes stem cell competition through EGFR signaling in the Drosophila testis. Sci. Rep 16 (9), 6118, 1.

Maqbool T, Soler C, Jagla T, Daczewska M, Lodha N, Palliyil S, VijayRaghavan K, Jagla K, 2006 Shaping leg muscles in Drosophila: role of ladybird, a conserved regulator of appendicular myogenesis. PloS One 1 (1), e122. [PubMed: 17205126]

McCloy RA, Rogers S, Caldon CE, Lorca T, Castro A, 2014 Partial inhibition of Cdk1 in G 2 phase overrides the SAC and decouples mitotic events. Cell Cycle 13, 1400–1412. [PubMed: 24626186]

Michailovici I, Harrington HA, Azogui HH, Yahalom-Ronen Y, Plotnikov A, et al., 2014 Nuclear to cytoplasmic shuttling of ERK promotes differentiation of muscle stem/progenitor cells. Development 141, 2611–2620. [PubMed: 24924195]

Michelson AM, Gisselbrecht S, Buff E, Skeath JB, 1998 Heartbroken is a specific downstream mediator of FGF receptor signalling in *Drosophila*. Development 125, 4379–4389. [PubMed: 9778498]

O 'Neill EM, Rebay I, Tjian R, Rubin GM, 1994 The activities of twoEts-related transcription factors required for Drosophila eye develop-ment are modulated by the Ras/MAPK pathway. Cell 78, 137–147. [PubMed: 8033205]

Pawlikowski B, Vogler TO, Gadek K, Olwin BB, 2017 Regulation of skeletal muscle stem cells by fibroblast growth factors. Dev. Dynam 246, 359–367.

Ren F, Wang B, Yue T, Yun EY, Ip YT, Jiang J, 2010 Hippo signaling regulates *Drosophila* intestine stem cell proliferation through multiple pathways. Proc. Natl. Acad. Sci. U.S.A 107, 21064–21069. [PubMed: 21078993]

Ross JJ, Duxson MJ, Harris AJ, 1987 Formation of primary and secondary myotubes in rat lumbrical muscles. Development 100, 383–394. [PubMed: 3652976]

Saito-Diaz K, Chen TW, Wang X, Thorne CA, Wallace HA, Page-McCaw A, Lee E, 2013 The way Wnt works: components and mechanism. Growth Factors 31, 1–31. [PubMed: 23256519]

Sarkissian T, Arya R, Gyonjyan S, Taylor B, White K, 2016 Cell death regulates muscle fiber number. Dev. Biol 415 (1), 87–97. [PubMed: 27131625]

Shilo BZ, 2014 The regulation and functions of MAPK pathways in Drosophila. Methods 68, 151–159. [PubMed: 24530508]

Stathopoulos A, Tam B, Ronshaugen M, Frasch M, Levine M, 2004 pyramus and thisbe: FGF genes that pattern the mesoderm of Drosophila embryos., 18(6), 687–699. Genes & Development 18 (6), 687–699. [PubMed: 15075295]

Sudarsan V, Anant S, Guptan P, VijayRaghavan K, Skaer H, 2001 Myoblast diversification and ectodermal signaling in Drosophila. Dev. Cell 1, 829–839. [PubMed: 11740944]

Swarup S, Verheyen EM, 2012 Wnt/Wingless signaling in Drosophila. Cold Spring Harb. Perspect. Biol 4, a007930. [PubMed: 22535229]

Takata H, Terada K, Oka H, Sunada Y, Moriguchi T, et al., 2007 Involvement of Wnt4 signaling during myogenic proliferation and differentiation of skeletal muscle. Dev. Dynam 236, 2800–2807.

Terada K, Misao S, Katase N, Nishimatsu S, Nohno T, 2013 Interaction of Wnt signaling with BMP/Smad signaling during the transition from cell proliferation to myogenic differentiation in mouse myoblast-derived cells. Int J Cell Biol 2013, 616294. [PubMed: 23864860]

Vincent S, Wilson R, Coelho C, Affolter M, Leptin M, 1998 The Drosophila protein Dof is specifically required for FGF signaling. Mol. Cell 2, 515–525. [PubMed: 9809073]

Vishal K, Bawa S, Brooks D, Bauman K, Geisbrecht ER, 2018 Thin is required for cell death in the Drosophila abdominal muscles by targeting DIAP1. Cell Death Dis. 3 (7), 740, 9.

Wu B, Li J, Chou Y-H, Luginbuhl D, Luo L, 2017 Fibroblast growth factor signaling instructs ensheathing glia wrapping of Drosophila olfactory glomeruli. Proc. Natl. Acad. Sci. U.S.A 114, 7505–7512. [PubMed: 28674010]

Xu N, Wang SQ, Tan D, Gao Y, Lin G, Xi R, 2011 EGFR, Wingless and JAK/STAT signaling cooperatively maintain Drosophila intestinal stem cells. Dev. Biol 354, 31–43. [PubMed: 21440535]

Yablonka-Reuveni Z, Rivera AJ, 1997 Proliferative dynamics and the role of FGF2 during myogenesis of rat satellite cells on isolated fibers. Basic Appl. Myol. BAM 7, 176–189.

Zappia MP, Frolov MV, 2016 E2F function in muscle growth is necessary and sufficient for viability in Drosophila. Nat. Commun 7, 10509. [PubMed: 26823289]

## Summary statement

We identify a novel role for FGF signaling in the regulation of myoblast proliferation in *Drosophila*. Our results indicate that FGF signaling upregulates nuclear β-catenin to control myoblast number.

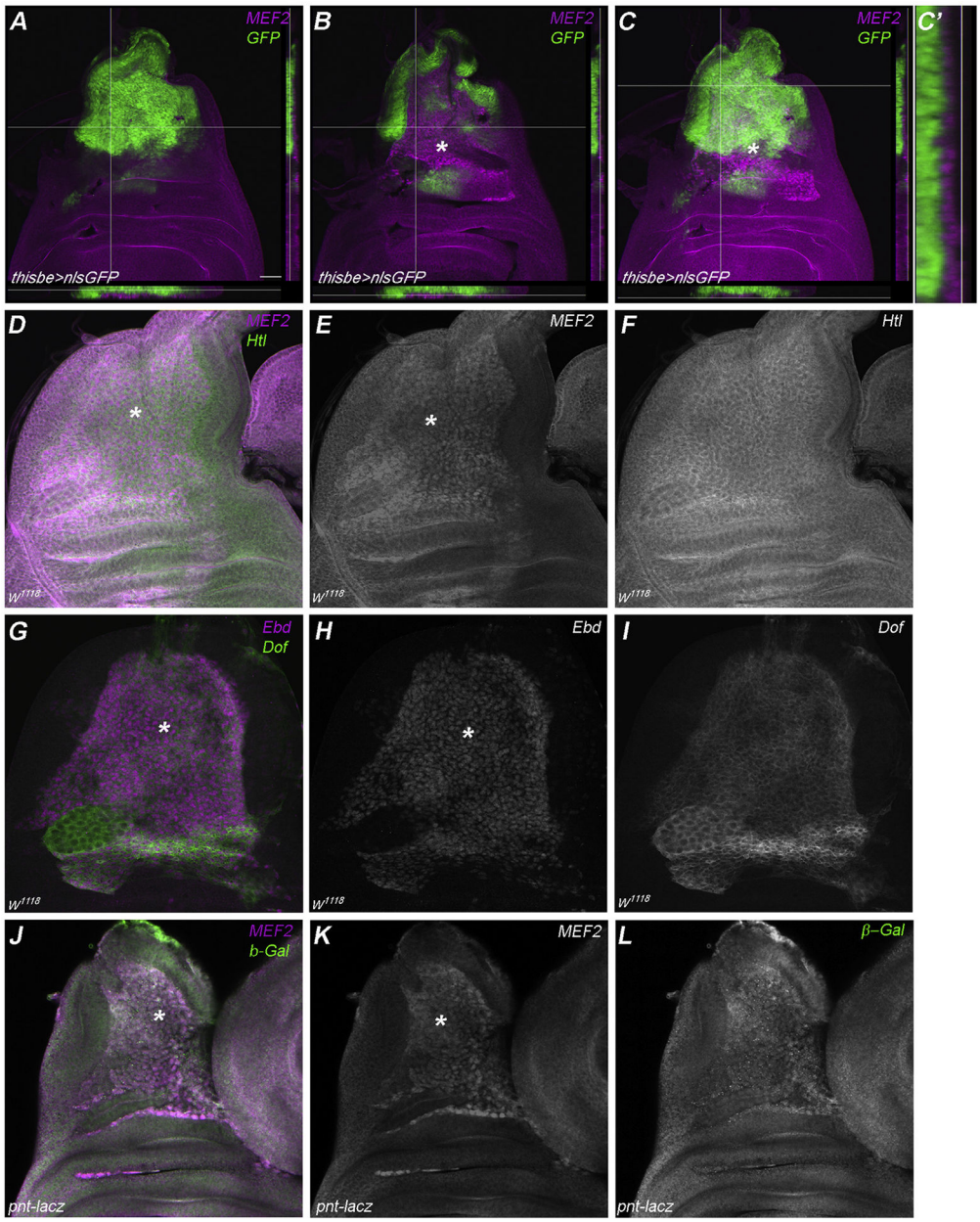


**Fig. 1.**

Components of the FGF signaling pathway are expressed in the wing imaginal disc. (A–C) Confocal micrographs showing late third instar wing discs from *ths* > *nlsGFP* animals, stained for accumulation of GFP (green) and MEF2 (magenta). Panel A has the notum as the focal plane, whereas panel B has the myoblasts of the same disc as the focal plane. Panel C and C' (magnified view) is a projection of multiple planes. Note that GFP is expressed in the wing disc epithelium (A, C, C′) and not in the myoblasts (B). (D–F) Wing disc associated myoblasts stained for accumulation of Htl (green) and MEF2 (magenta). Htl accumulation is observed around MEF2 positive myoblast nuclei. (G–H) Accumulation of Dof (green) is observed in the adult myoblasts (magenta). (J–L) Confocal micrographs depicting *pointed-lacz* (*pnt-lacZ*) expression in adult myoblasts. Single optical section of imaginal wing disc

showing co-localization of β-gal (green) and MEF2 (magenta) (J–L). (*) represents myoblast location. Scale bar, 20 μm.

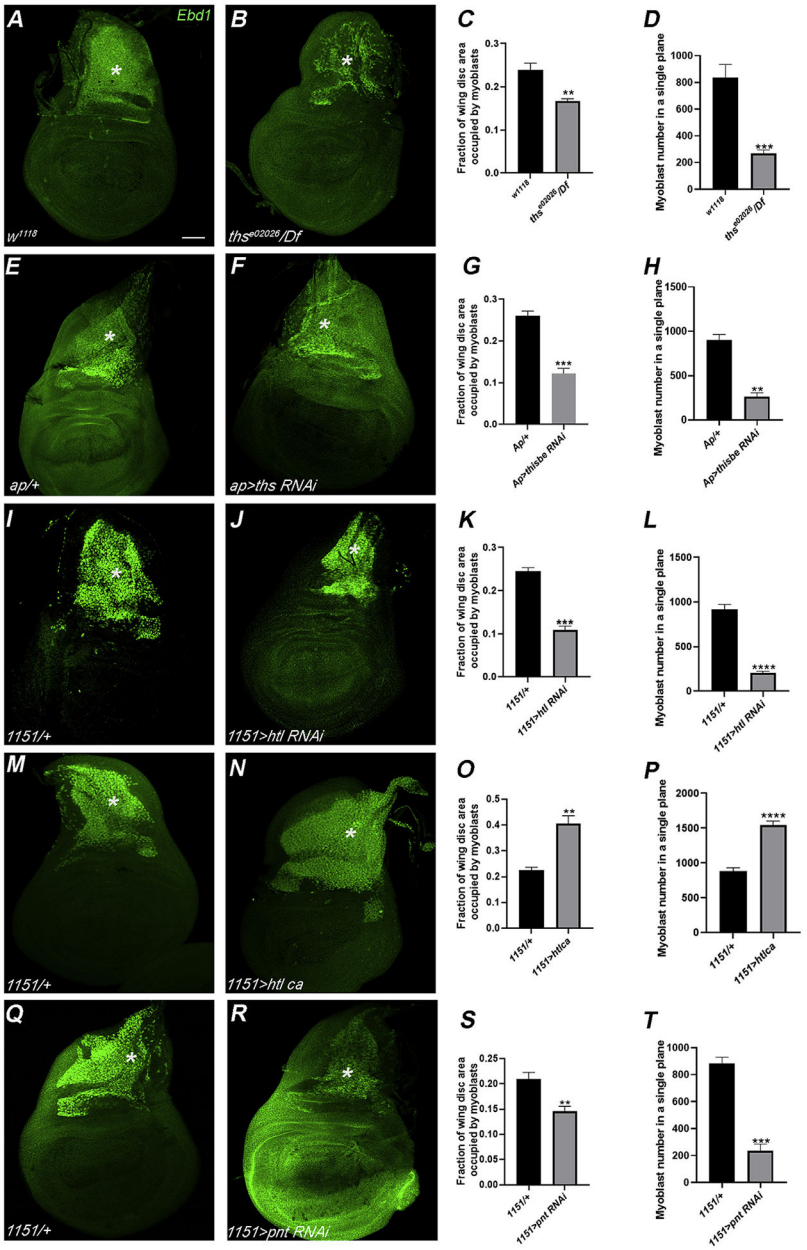


**Fig. 2.**

FGF signaling regulates myoblast pool size. (A–H) Confocal images showing the effect on myoblast number of disrupting *ths* expression. (A, B) *ths* mutants have fewer myoblasts as compared to control. (C, D) Quantification of myoblast area (proportion of the area containing myoblasts compared to the total area of the disc) and number (calculated as the total number of myoblasts in the confocal plane with the largest myoblast area) in controls and *ths* mutant flies. (E–H) Knockdown of *ths* function in the wing epithelium reduces myoblast area and pool size. (I–L) Abrogating *htl* expression results in a reduced myoblast population as compared to control. (M–P) Effects of activating Htl signaling on wing disc associated myoblasts. Note that there is a significant increase in area and number of myoblasts in *1151 > htl ca* samples as compared to control. (Q–T) Knockdown of *pnt*

reduces myoblast area and number. (*) represents myoblast location. Note that myoblasts are distributed in different shapes among different samples. Scale bar, 50 μm.

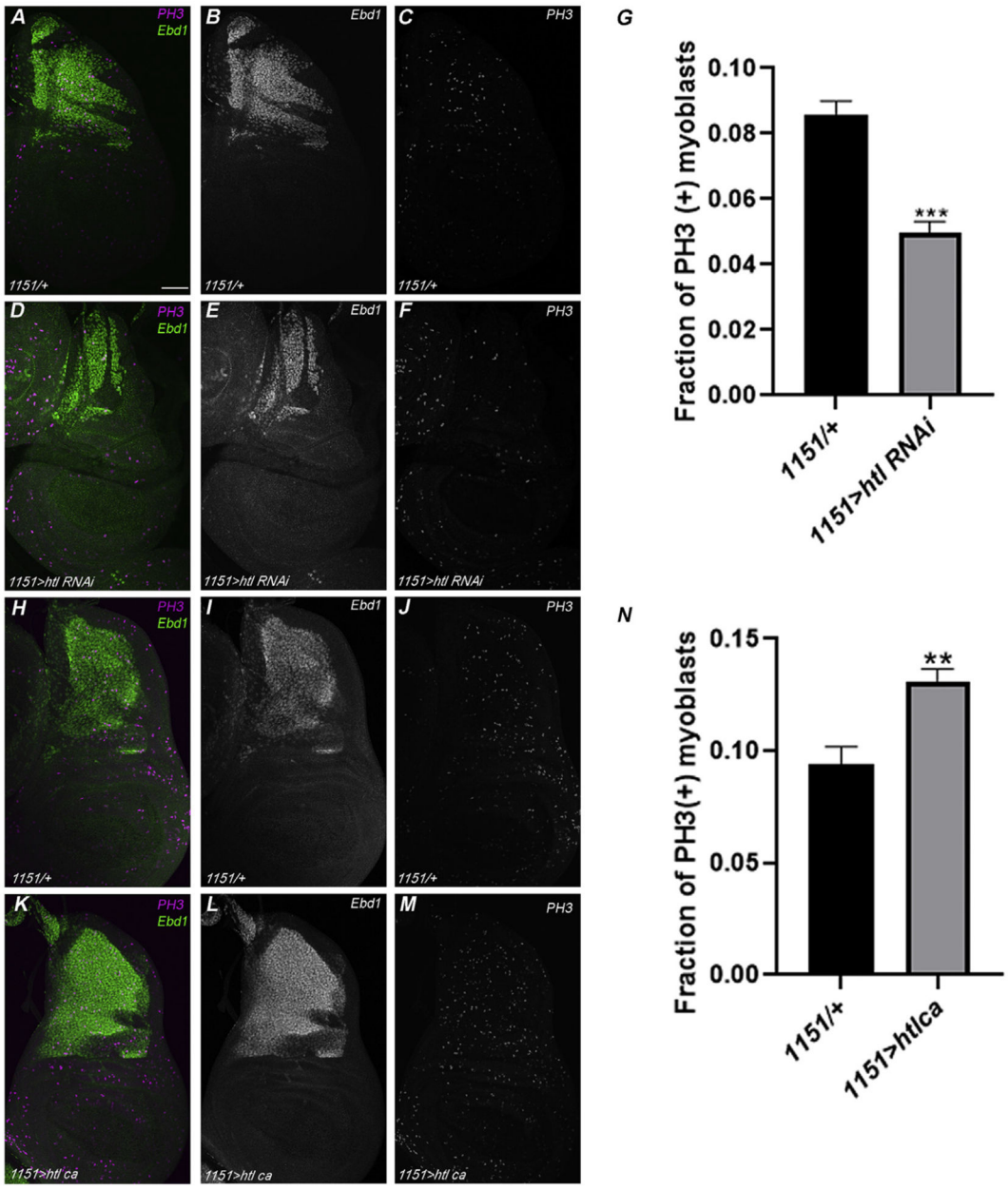


**Fig. 3.**

Htl controls myoblast proliferation. (A–G) Effects of blocking Htl on myoblast proliferation. (A–F) Wandering third instar larval wing disc associated myoblasts double stained for Ebd1 (green) and PH3 (magenta) in control (A–C) and *1151 > htl RNAi* flies (D–F). (G) Quantification showing significantly fewer PH3 positive myoblasts in *1151 > htl RNAi* samples as compared to the controls. (H–M) Compared to controls (H–J), *1151 > htl ca* flies (K–M) have a higher proportion of PH3 positive adult myoblasts. (N) Bar graph showing significantly higher fraction of proliferating myoblasts in *1151 > htl ca* flies. Images shown are single confocal sections. Scale bar, 50 μm.

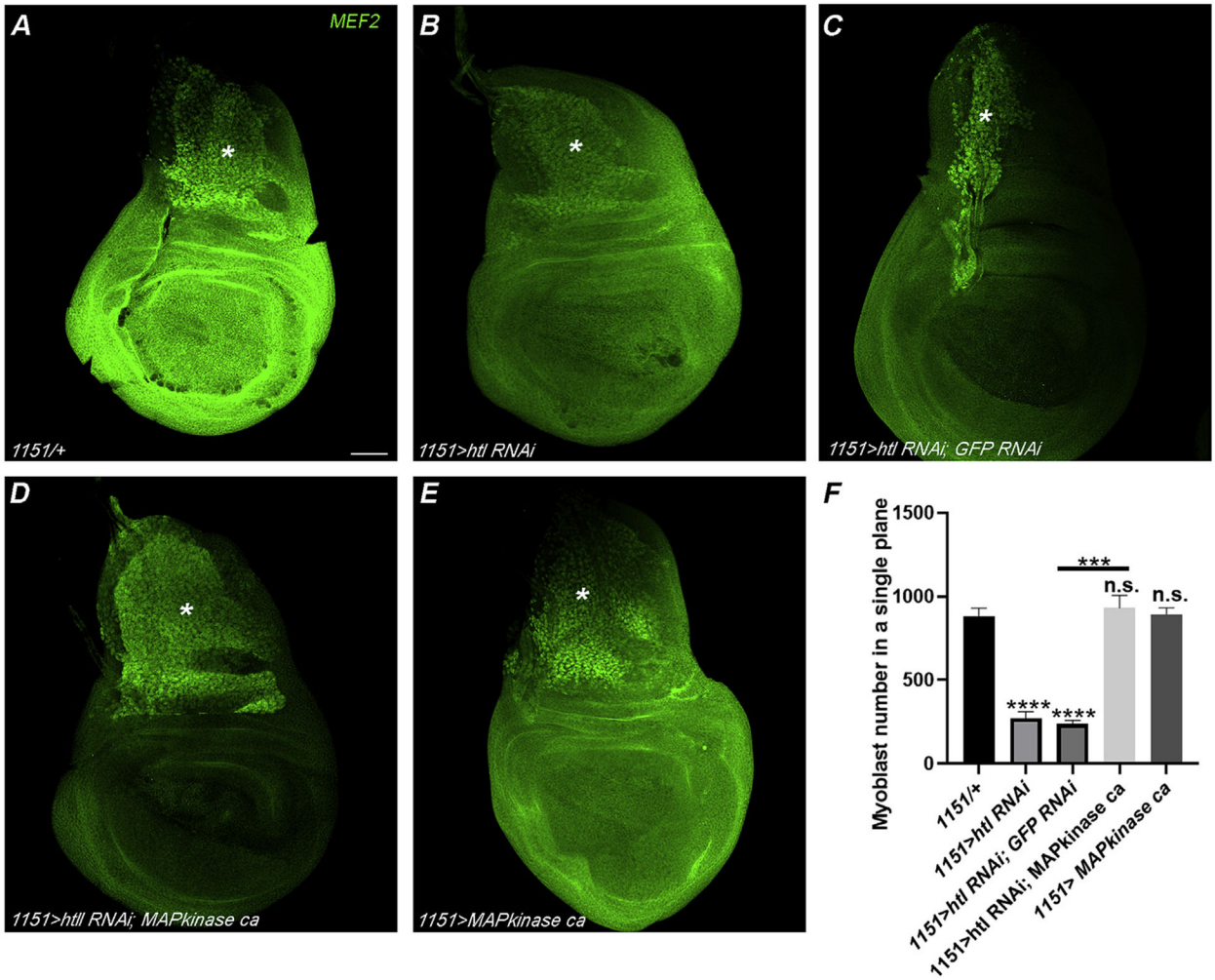


**Fig. 4.**

Expression of activated MAP kinase rescues myoblast pool size in *1151 > htl RNAi* flies. Late third instar larval wing disc associated myoblasts stained for accumulation of MEF2, in control (A), *1151 > htl RNAi* (B), *1151 > ; htl RNAi; GFP RNAi* (C), *1151 > htl RNAi; MAPKinase ca* (D) and *1151 > MAPKinase ca* (E) samples. (F) Bar graph showing rescue of myoblast pool size between control and *1151 > htl RNAi; MAPKinase ca* flies. (*) represents myoblast location Scale bar, 50 μm.

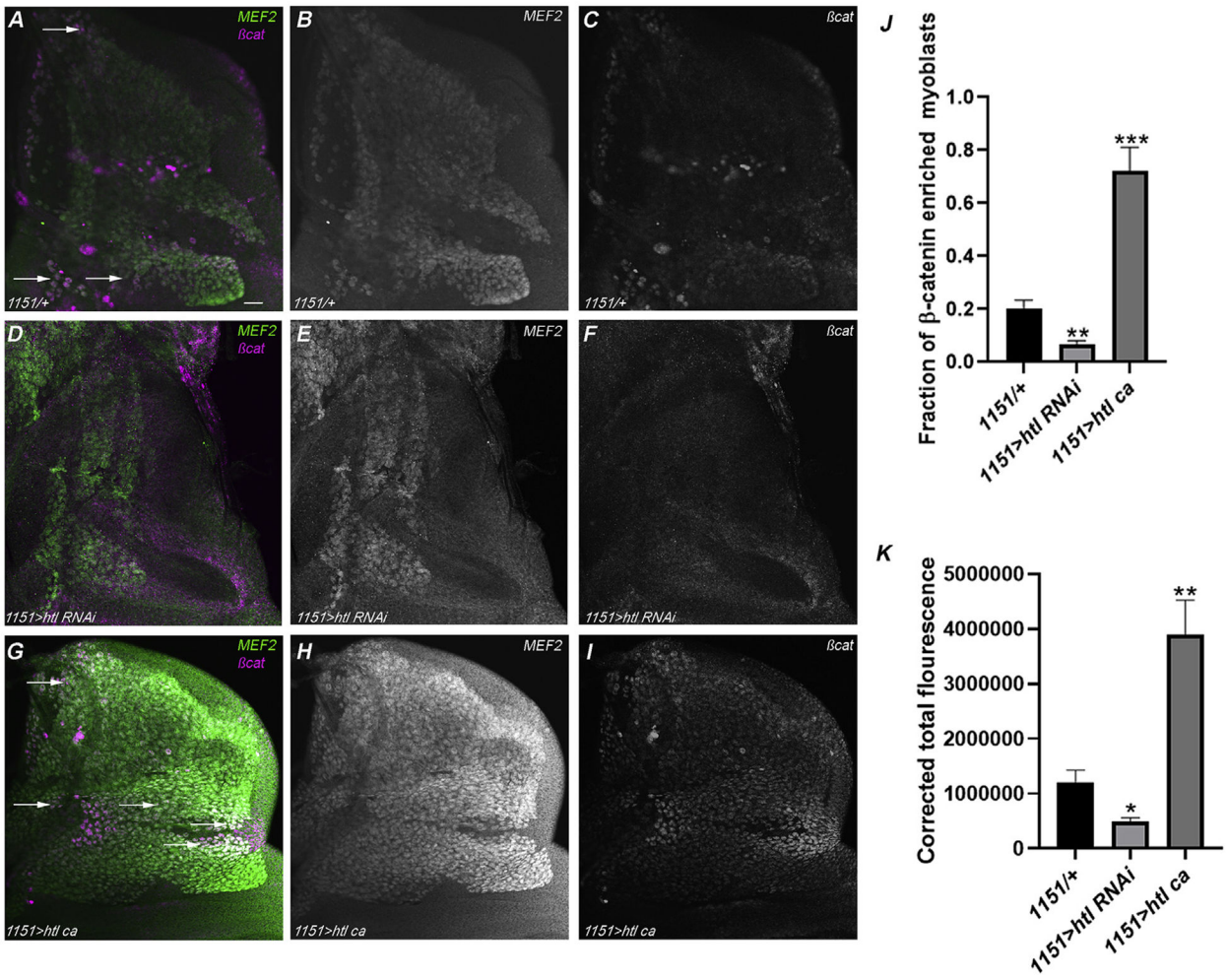


**Fig. 5.**

Htl activates β catenin activity to regulate myoblast pool size. Confocal micrographs of third larval instar wing imaginal discs stained for MEF2 (green) and βcat (magenta). (A–C) There is a modest number of myoblasts with nuclear-enriched βcat in the wing disc in control samples (arrows). (D–F) There are hardly any βcat positive myoblasts in *1151 > htl RNAi* discs. (G–I) *1151 > htl ca* flies show nuclear accumulation of βcat in a large number of myoblasts (arrows). (J) Quantification showing a significantly smaller fraction of βcat-positive myoblast nuclei in *1151 > htl RNAi* samples, whereas *1151 > htl ca* discs have a higher proportion of βcat-positive myoblasts as compared to controls. (K) Quantification of βcat fluorescent intensities indicates a significant reduction in nuclear βcat levels in *1151 > htl RNAi* and an increase in nuclear βcat levels in *1151 > htl ca* samples as compared to controls. Scale bar, 20 μm.

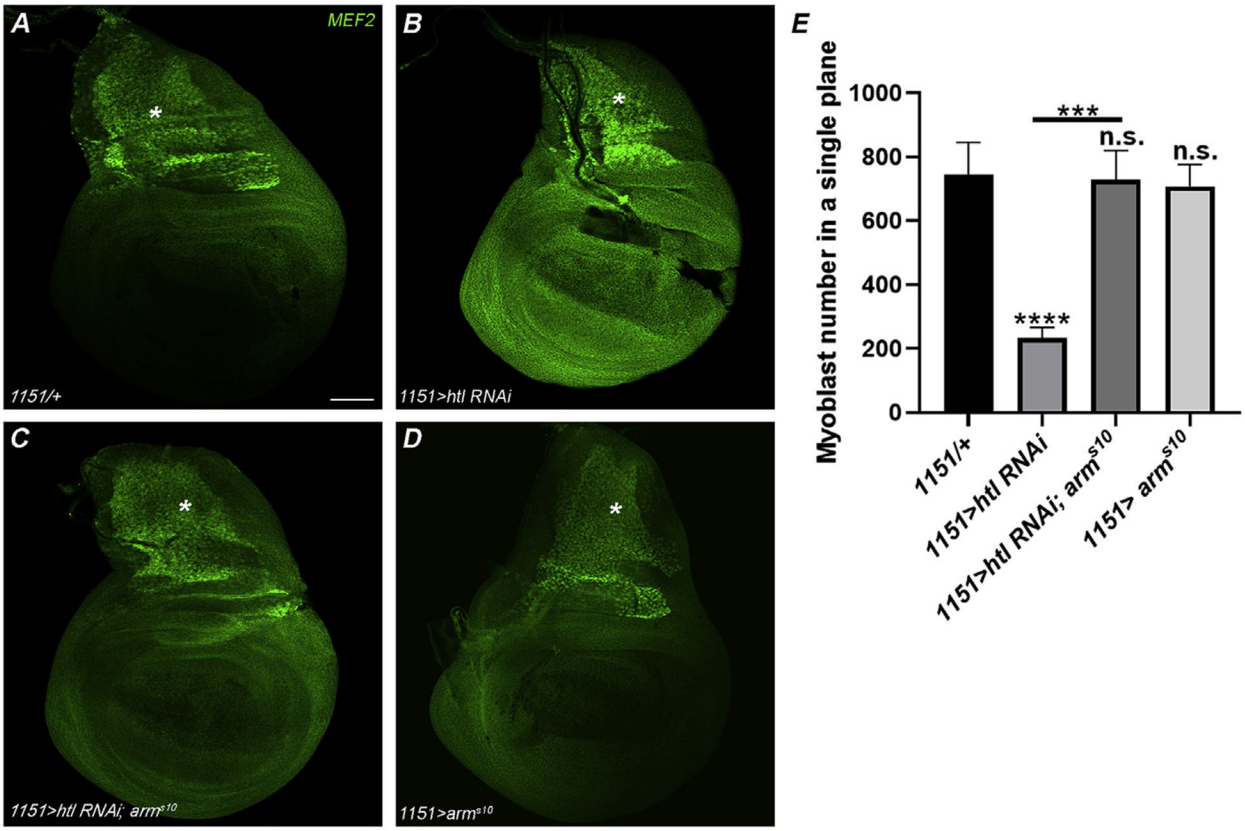


**Fig. 6.**

Armadillo acts downstream of Htl to regulate myoblast number. Late third instar larval wing imaginal discs of control (A), *1151 > htl RNAi* (B), *1151 > htl RNAi; arm$^{S10}$* (C), and *1151 > arm$^{S10}$* (D), stained for accumulation of MEF2. (E) Quantification of the myoblast pool in a single plane revealed no significant difference between control and *1151 > htl RNAi; arm$^{S10}$* samples. (*) represents myoblast location Scale bar, 50 μm.